Supporting Information

Mateos-Gil et al. 10.1073/pnas.1204844109

SI Text

Filament Shape Parametrization. For each atomic force microscopy (AFM) image, the height of every pixel (z) was read and the average ($\langle z\rangle$) and standard deviation (σ_z) calculated, discarding all pixels below the threshold level $h_{\text{threshold}} = \langle z\rangle + 2\sigma_z$. The selected pixels were then grouped in clusters larger than 25 pixels. Smaller clusters were discarded because they often corresponded to static blobs of protein. The clusters selected described the protein strands. Once these filaments were identified, the center of mass of the clusters was calculated and used as center for the polar coordinate expressed by the pairs $\{(r_i, \theta_i)\}_{i=1}^{N}$, being N the number of clusters. In this coordinate system, we can describe the filament with a harmonics series

$$r(\theta) = \frac{1}{2}a_0 + \sum_{n=1}^{5}[a_n \cos(n\theta) + b_n \sin(n\theta)]. \qquad \textbf{[S1]}$$

The series is truncated at the fifth term in order to have enough flexibility to adjust any filament. The fitting procedure provides the values for the coefficients (a_n, b_n) that minimize the function D^2:

$$D^2 = \sum_{i=1}^{N}[r_i - r(\theta_i)]^2 + \epsilon \sum_{n=1}^{5} n^3(a_n^2 + b_n^2). \qquad \textbf{[S2]}$$

The first term is the contribution of the square distance between the pixel clusters and the fitted curve, and the second is a contribution that penalizes the higher order harmonics to avoid overfitting by high-frequency oscillations. The weight of this second contribution relative to the first one is determined by the parameter ϵ. It was chosen to be $\epsilon = 0.1$, but there were no detectable differences in the fitted curve for small variations in ϵ. This analysis can also be applied to open filaments if the θ value is restricted to a limited range. Fig. S1 illustrates that the procedure gives a smooth and fairly accurate fit of the open filaments (Fig. S1*A*) and the closed rings (Fig. S1*B*). The integration of the analytical curve $r(\theta)$ provides the filament length at each frame. Fig. S1*C* shows the time evolution of the length of a given filament $L(t)$.

Statistical Analysis of Filamenting Temperature-Sensitive Mutant Z (FtsZ) Polymers at Single-Filament Level. AFM images provide information on individual FtsZ filaments. The survival time of each closed FtsZ rings (Fig. 4 in the main paper) and the decay in length with time of open filaments (Fig. 5 in the main paper) can be measured directly. These experimental data are beyond the usual description of the chemical reaction kinetics, which analyzes the average depolymerization in a large ensemble of filaments, disregarding their size distribution. Here we use simple examples to illustrate the statistical methods that are used to extract all the information provided by the *single-filament* data from AFM images.

For the analysis of closed rings, our experimental results show clearly that the ring survival time depends on ring size. On average, large rings disappear sooner than small rings. A coarse description within the framework of the kinetics of chemical reactions would add all the observations together, to get a lifetime distribution with a corresponding mean lifetime, which would depend on the particular distributions of ring sizes. However, with the statistical treatment described in the section below, we can check the hypothesis that the reaction rate for the irreversible depolymerization is proportional to the ring size, and get a breaking rate per bond that is independent of ring length. This information can then be "exported" to the analysis of open filaments.

For the depolymerization velocity of open filaments (Fig. 5 in the main paper), our analysis goes beyond the usual reaction kinetics concerned with mean values in systems with a large number of molecules. We use the tools of the statistical physics of small systems to analyze the fluctuations of depolymerization velocity around its mean value. This analysis is crucial to extract all the information provided by the single-filament data from AFM images, as demonstrated below in the simple example in *Statistical distribution for the instantaneous depolymerization velocities of single FtsZ filaments*.

Analysis of the lifetimes for FtsZ closed rings with different sizes (collective kinetics for multiple reactions with proportional rates). Considering FtsZ rings in the sample and their irreversible depolymerization a process triggered by a single reaction with a rate v_o in a purely random way, then the time evolution equation for the concentration of these rings $Z_{\text{rings}}(t)$ would be

$$\frac{dZ_{\text{ring}}(t)}{dt} = -v_o Z_{\text{ring}}(t), \qquad \textbf{[S3]}$$

and its solution would give the number of rings at any time as

$$Z_{\text{ring}}(t) = Z_{\text{ring}}(0)\exp(-v_o t). \qquad \textbf{[S4]}$$

The mean survival time of a ring could be calculated as

$$\langle T\rangle = \frac{\int_0^\infty T Z_{\text{ring}}(t)dt}{\int_0^\infty Z_{\text{ring}}(t)dt} = \frac{\int_0^\infty T e^{-v_o t}dt}{\int_0^\infty e^{-v_0 t}dt} = v_o^{-1}, \qquad \textbf{[S5]}$$

so that the reaction rate v_o could be obtained directly from the mean survival times of the rings. If our experimental data (presented in Fig. 4 of the main paper) were analyzed in this way, distinguishing as different populations of rings the ones grown under different experimental conditions, we would get $\langle T\rangle = 6.45$ min for GTP in the normal buffer, $\langle T\rangle = 13.13$ min for GMP, and $\langle T\rangle = 8.88$ min for GTP with 15% glycerol; giving reaction rates $v_o = 0.15$, 0.076, and 0.11 per minute, respectively. That would be the only information available from the experimental data with the simple analysis of the irreversible depolymerization as a single random process over the whole experimental sample.

However, there is more information contained in these datasets. In Fig. S2 we present the (normalized) distribution for the observed times for FtsZ rings, in terms of the reduced time $\tau = T/\langle T\rangle$ for each buffer condition. According to Eqs. **S4**, **S5**, this distribution should be a pure exponential, $P(\tau) = \exp(-\tau)$, but the experimental results seem to deviate from that simple form.

The statistics are not very good, because the number of rings is not very large, but (because we have already normalized the times in each dataset with its own mean value), we may accumulate the three sets in the single histogram. The better quality of the accumulated histogram confirms the nonexponential shape of $Z_{\text{rings}}(t)$: The decay is too rapid at short times and too slow at the tail of the distribution.

This representation of the experimental data shows that the depolymerization of the rings cannot be described by a single

reaction rate v_o to represent all the rings in each sample. We have to look for the additional elements that explain why the depolymerization of the rings deviates from the simple behavior defined by Eq. **S3**. The experimental data provide the length of individual rings. This information is very useful because its shows clearly that longer rings disappear faster than smaller ones. Having a mixture of rings with different sizes gives a complex (nonexponential) behavior to the time-decay of the total population of rings.

Let us consider two subpopulations of FtsZ rings, Z_a and Z_b, shrinking through different reaction rates v_a and v_b, respectively (e.g., because they have different sizes $N_b = 2N_a$, and that is reflected in $v_b = 2v_a$). The concentrations of each component would follow a simple exponential decay $Z_a(t) = Z_a(0)\exp(-v_a t)$ and $Z_b(t) = Z_b(0)\exp(-v_b t)$, but if we treat all of them together, the total number of rings $Z_{\text{rings}}(t) = Z_a(t) + Z_b(t)$, evolves like

$$Z_{\text{rings}}(t) = Z_a(0)\exp(-v_a t) + Z_b(0)\exp(-v_b t), \qquad \textbf{[S6]}$$

which does not follow the simple Eq. **S3**.

If we describe the full sample as a whole, the mean survival time would be

$$\langle t\rangle = \frac{v_a^{-2}Z_a(0) + v_b^{-2}Z_b(0)}{v_a^{-1}Z_a(0) + v_b^{-1}Z_b(0)}, \qquad \textbf{[S7]}$$

which depends on the initial amount of rings of each type, $Z_a(0)$ and $Z_b(0)$, and which gives some intermediate value between the two reactions rates v_a and v_b that really describe the depolymerization process in the sample. Fig. S3, *Left* shows the shape of $Z_{\text{rings}}(t)$ compared with the exponential form $P(\tau) = \exp(-\tau)$ of a single process with the same mean value $\langle t\rangle$ as given by [**S7**]. The deviation of $Z_{\text{rings}}(t)$ from the exponential shape is similar to that observed in Fig. S2 for the actual experimental results.

Obviously, in this example, we may do separate analysis of the data for the two subpopulations, to recover the simple exponential distribution for each one, $Z_a(t) = Z_a(0)\exp(-v_a t)$ and $Z_b(t) = Z_b(0)\exp(-v_b t)$, so that the complex stochastic phenomena behind $Z_{\text{rings}}(t)$ is decomposed in its simple components. However, if we have some hypothesis for the ratio between the two reaction rates v_b/v_a (e.g., we may guess that the reaction for b is twofold faster than for a because b rings are twice as large as the a rings), we may check the accuracy of the hypothesis defining effective times, $t_{\text{ef}} = 2t$ for a and $t_{\text{ef}} = t$ for b, and collecting the information of $Z_a(t)$ and $Z_b(t)$ into a single function for equal values of their effective times, $Z_{\text{ef}}(t) = Z_a(2t) + Z_b(t)$. The result, presented in Fig. S3, *Right*, is

$$\begin{aligned} Z_{\text{ef}}(t) &= Z_a(0)e^{-2v_a t} + Z_b(0)e^{-v_b t} = [Z_a(0) + Z_b(0)]e^{-2v_a t} \\ &= Z(0)e^{-2v_a t}, \end{aligned} \qquad \textbf{[S8]}$$

which follows the simple Eq. **S3** with a single effective rate $v_{ef} = 2v_a$. Therefore, the basic hypothesis $v_b = 2v_a$ would then be confirmed (or rejected) by the observation (or not) of a pure exponential shape for the distribution of reduced survival times $\tau = t_{\text{ef}}/\langle t_{\text{ef}}\rangle$.

This procedure becomes very useful if, instead of the two components a and b, we have a stochastic process with many simple components, each with a different reaction rate v_N. That is the case for the irreversible breaking of FtsZ rings with a broad initial distribution of size $P_N(0)$, which would evolve in a complex way,

$$Z_{\text{rings}}(t) = \sum_N P_N(0)\exp(-v_N t), \qquad \textbf{[S9]}$$

adding to the nonexponential decay in Fig. S2. The separated analysis of each ring population, $Z_{\text{ring}}(t)$, would be impossible because we do not have enough observations for each value of N, so that we lack information to get accurate separated fits to $Z_{\text{N}}(t) = P_{\text{N}}(0)\exp(-v_{\text{N}}t)$. However, the obvious hypothesis to be tested is that the reaction rates for depolymerization are proportional to the length of each ring, so that, as described above, we define the effective time of a ring with length N as $t_{\text{ef}} = Nt$. As shown in Fig. 4 of the main paper, this description leads to the simple exponential decay of $P(t_{\text{ef}}/\langle t_{\text{ef}}\rangle)$, so that the hypothesis is confirmed: The irreversible depolymerization of FtsZ rings is triggered by independent events at each bond, so that the reaction rate v_o is proportional to N, and the whole process is described by a single reaction rate per bond $v_o = \langle t_{\text{ef}}\rangle^{-1}$, which characterizes all the rings in each nucleotide buffer.

Statistical distribution for the instantaneous depolymerization velocities of single FtsZ filaments. If we consider the simplest depolymerization process, where monomers are released from a filament one-by-one by a purely stochastic process with fixed rate v, then the change of the number of FtsZ filaments with length N, $Z_N(t)$, in a sample with a broad size distribution is given by the reaction kinetic equation

$$\frac{dZ_N(t)}{dt} = -vZ_N(t) + vZ_{N+1}(t) \qquad \textbf{[S10]}$$

for $N \geq 2$. The integration of these coupled equations gives the populations $Z_N(t)$ from the set of initial values $Z_N(0)$, and we could extract any global measure of the sample, like the total number $Z_{\text{tot}}(t)$ and the total length of all the filaments $L_{\text{tot}}(t)$ as

$$Z_{\text{tot}}(t) = \sum_{N\geq 2} Z_N(t), \qquad \textbf{[S11]}$$

$$L_{\text{tot}}(t) = \sum_{N\geq 2} NZ_N(t), \qquad \textbf{[S12]}$$

then the total mean length of the filaments in the sample is given by

$$\langle N\rangle(t) = \frac{\sum_{N\geq 2} NZ_N(t)}{\sum_{N\geq 2} Z_N(t)} = \frac{L_{\text{tot}}(t)}{Z_{\text{tot}}(t)}. \qquad \textbf{[S13]}$$

If we may neglect the adsorbing boundary at the short filament end of the distribution $Z_N(t)$ (i.e., as far as all the initial filaments still have $N > 2$), the total number of filament is constant

$$\frac{dZ_{\text{tot}}(t)}{dt} = -v\sum_N Z_N(t) + v\sum_N Z_{N+1}(t) = 0, \qquad \textbf{[S14]}$$

and the mean length decays steadily at the rate v

$$\frac{d\langle N\rangle(t)}{dt} = -v\frac{\sum_{N\geq 2} N[Z_N(t) - Z_{N+1}(t)]}{Z_{tot}(t)} = -v\frac{Z_{\text{tot}}(t)}{Z_{\text{tot}}(t)} = -v, \qquad \textbf{[S15]}$$

$$\langle N\rangle(t) = -vt \qquad \textbf{[S16]}$$

as it may have been written directly, because all the filaments are shrinking at that mean rate. Therefore, the depolymerization rate v could be directly extracted from experimental observations for the mean decay of the filament length (i.e., the mean depolymerization velocity) as

$$\langle V\rangle = \frac{\langle N\rangle(t_f) - \langle N\rangle(t_0)}{t_f - t_0} = -v. \qquad \textbf{[S17]}$$

However, the information obtained experimentally by the estimation $\langle V\rangle$ is not enough to characterize the depolymerization mechanism. If we consider a four-by-four mechanism (i.e., depolymerization occurs taking off pieces of four monomers from the filament with a rate v'), the reaction kinetics would be described now by

$$\frac{dZ_N(t)}{dt} = -v'Z_N(t) + v'Z_{N+4}(t), \qquad \textbf{[S18]}$$

and we may follow the same argument as above to get the mean depolymerization rate as

$$\frac{d\langle N\rangle(t)}{dt} = -v'\frac{\sum_{N\geq 2} N[Z_N(t) - Z_{N+4}(t)]}{Z_{\text{tot}}(t)} = -v'\frac{4Z_{\text{tot}}(t)}{Z_{\text{tot}}(t)} = -4v', \qquad \textbf{[S19]}$$

$$\langle V\rangle = \frac{\langle N\rangle(t_f) - \langle N\rangle(t_0)}{t_f - t_0} = -4v', \qquad \textbf{[S20]}$$

therefore $\langle V\rangle$ cannot be used to discern between a basic depolymerization mechanism that releases the monomers, one-by-one, at a rate $v \equiv v_1$, and another mechanism in which the monomers are released in bunches of four monomers but fourfold slower—i.e., with a rate $v' \equiv v_4 = v_1/4$. Moreover, any stochastic combination of both processes could be interpreted either as a one-by-one or a four-by-four mechanism.

As will be shown below, analysis of the distribution of instantaneous velocities can distinguish between the two depolymerization mechanisms described above. Notice that the principal advantage of AFM is that we get direct access to the time evolution of single filaments and it is possible to construct the whole instantaneous velocities histogram between two AFM frames. In contrast, such information is not accessible from any other experimental method that looks at ensembles and collects the mean size value from a broad distribution of filament lengths.

For a set of images of one filament taken at Δ_t intervals, we get a time series $N(t_i)$ for $t_i = i\Delta_t$, and $i = 0, 1, 2, \ldots$. The depolymerization velocity in each time interval is given by

$$V(t_i) = \frac{N(t_{i+1}) - N(t_i)}{\Delta_t} \qquad \textbf{[S21]}$$

then, in the one-by-one monomer depolymerization mechanism with a rate v, the observed velocities would be $V = 0, 1/\Delta_t, 2/\Delta_t, 3/\Delta_t, \ldots, n/\Delta_t$ that correspond to have 0, 1, 2, 3,…, n releasing events in the time interval $t_{i+1} - t_i = \Delta_t$. The probability for each possible value of V is given by a Poisson distribution

$$P\left(V = \frac{n}{\Delta_t}\right) = \frac{e^{-v\Delta_t}(v\Delta_t)^n}{n!}. \qquad \textbf{[S22]}$$

In contrast, with a depolymerization in bunches of four monomers with rate $v' = v/4$ would produce only values $V = 0, 4/\Delta t, 8/\Delta t, \ldots$, with probabilities

$$P\left(V = \frac{4n}{\Delta_t}\right) = \frac{e^{-v'\Delta_t}(v'\Delta_t)^n}{n!}. \qquad \textbf{[S23]}$$

The mean value of n from **[S22]** would be $\langle n\rangle = v\Delta_t$, so that the mean depolymerization velocity is $\langle V\rangle = \frac{\langle n\rangle}{\Delta_t} = v$, as expected. Similarly, from **[S23]** we get $\langle n\rangle = v'\Delta_t$, so that the mean depolymerization velocity is $\langle V\rangle = \frac{4\langle n\rangle}{\Delta_t} = 4v' = v$. The two processes would give again the same mean depolymerization velocity, but now we may easily discern between the two alternatives from the very different shape probability distributions (Fig. S4).

In particular, the typical deviation for the velocity distributions would be $\sigma_V \equiv \sqrt{\langle V^2\rangle - \langle V\rangle^2} = \sqrt{v/\Delta_t}$ from **[S22]** and $4\sqrt{v'/\Delta_t} = 2\sqrt{v/\Delta_t}$ from **[S23]**—i.e., with equal values of $\langle V\rangle = v$, the typical deviation in the four-by-four depolymerization mechanism would give twofold larger than for the one-by-one. Therefore, the experimental estimation of $\langle V\rangle$ and σ_V would provide the information to discern between depolymerization processes. Moreover, if we can get accurate results for the whole probability distribution $P(V)$, and it shows a non-Poissonian shape as in Fig. 6 in the main article, we would learn that the polymerization reaction follows a more complex reaction pattern than a mixture of one-by-one, four-by-four, or other unbiased depolymerization steps. In this case of such a sized-biased process, to get an analytical prediction of $P(V)$, the use of computer simulations (with simple parametric forms for the size dependence of the fragmentation rates) provides the simplest way to compare with the experimental distributions.

To conclude, notice that the method is still valid for relatively long time intervals (in the series of AFM images we have $\Delta_t \approx 1$ min), so that $v\Delta_t$ may be relatively large (approximately 10 in our case) and the observed depolymerization steps are usually composed of several basic steps. The probability distributions **[S22, S23]** are still valid, although for large Δ_t, they become narrower, $\sigma_V \sim 1/\sqrt{\Delta_t}$, and it would be more difficult to discern the shape. Also, there is an inherent noise from the imaging and the parametrization of the filaments, to get $N(t)$, so that the hypothetical probability distributions $P(V)$ are blurred, and we even observe some positive values of V (spurious polymerizations from the uncertainty in the experimental characterization of the filament length). Nevertheless, we have proved here that, with a feasible number of observations, we may get enough resolution in $P(V)$ to discard both a one-by-one depolymerization and the unbiased fragmentation.

Langevin Computer Simulations. Protein monomers are modeled as beads of a chain linked by elastic springs that give an optimal distance between beads and an optimal angle between bonds, with thermal fluctuations around these optimal values, assuming that each protein monomer moves in a viscous fluid, with limiting velocity proportional to the instantaneous force. The force on each monomer has a deterministic component coming from the springs that links it to its neighbors along the chain, and a stochastic component that represents the thermal noise—i.e., the molecular collisions with the bath.

The characteristics of the springs and the thermal bath were tuned to reproduce the distribution of filament shapes observed in AFM images for short FtsZ filaments, polymerized with a slowly hydrolyzing GTP analogue (1). A computer simulation using this same model may be used to describe the separation

of the filaments fragments following the elimination of one of the spring bonds, to mimic the breaking of a bond along the chain.

Size-dependent diffusion effect of FtsZ filament fragments. We have simulated the breaking of open filaments with $N = 100$ monomers each. The initial shapes of the filaments were selected along the configurations of a long Langevin simulation in thermal equilibrium at room temperature. For each of these configurations, a bond was broken, either at the middle point, breaking the filament in two parts with $N_a = N_b = 50$ each, or at one end of the filament, separating a single monomer $N_a = 1$ from the remaining $N_b = 99$ monomers. At the breaking time, the monomers started with their original (bounded) coordinates, but the spring joining them was deleted to simulate the effect of the GTP hydrolysis. Then the simulation was run for the two fragments of the filament, to follow the time evolution of distance and relative angular orientation between the two previously associated monomers. These variables follow a Brownian diffusive dynamics, so that the distance and the angular mismatch change in a random way but, on average, they move away from their initial values as shown in Fig. S5. The main difference between the diffusion of an isolated monomer and that of a monomer still linked to a longer filaments appears in the relative angle $\Delta\phi$ between their orientations. It increases more than threefold only 0.1 s after rupture.

The timescale for the Langevin simulation has been calibrated from the comparison of the fluctuations in the shape of closed rings observed in AFM images and in Langevin simulations with the same model. According to the hydrolysis rate for GTP, approximately 8 min^{-1}, the FtsZ bonds become weaker every 7 to 8 s, and they would open to replace the GDP by a fresh GTP from solution. The small time fraction of (*ca.* 0.05–0.1 s) needed for that replacement would be enough to produce an important angular mismatch in the orientation of an isolated monomer, so that after capturing a GTP, the FtsZ monomer may diffuse away from the remaining filament, instead of finding its way to remake the broken bond. In contrast, when the breaking of the filament leaves two large fragments, their typical diffusion during the same time would be of only a few degrees of angular mismatch (and a few nanometers of distance), making more likely that the bond is sealed after the nucleotide exchange. Notice that a quantitative estimate for the frequencies of the depolymerization reaction rates would require a description of the GTP hydrolysis and replacement at the molecular level, and the above estimations can only be used at a qualitative level because support to the hypothesis that the fragmentation rate may depend on the fragment size.

1. Hörger I, et al. (2008) Langevin computer simulations of bacterial protein filaments and the force-generating mechanism during cell division. *Phys Rev E Stat Nonlin Soft Matter Phys* 77:011902.

Size biased fragmentation process for FtsZ filaments. We have run computer simulations for the fragmentation of 10^5 filaments, with initial sizes following the distribution observed for closed rings (Fig. 1 in the main paper), assuming that a filament with size $\langle N_o \rangle$ may undergo any possible fragmentation in two pieces of size N_a and $N_b = N_o - N_a$, but with a frequency that depends on the size of the fragments.

$$v(N_a, N_b) = v_o + v_1(e^{-N_a/L} + e^{-N_b/L}). \qquad \textbf{[S24]}$$

The parameter v_1 represents the rupture frequency of short filaments (i.e., with size $N_{a,b} \ll L$), whereas the value of v_o gives the breaking frequency of long fragments (i.e., with size $N_{a,b} \gg L$). Fragmentations are attempted at randomly chosen points and accepted with a probability $P(N_a, N_b)$ proportional to $v(N_a, N_b)$. As done in the analysis of the experimental depolymerization histories, after a fragmentation, we keep track only of the larger segment of the filament, so that we cut away a bunch of $N_{\text{cut}} = \min(N_a, N_b)$ monomers, and iterate the process until the larger fragment becomes shorter than 10 monomers.

The value of v_o is keep to be the irreversibly opening frequency obtained from the analysis of closed rings (Table 1 in the main paper), whereas v_1 and L are used to get the same mean value and asymmetry of the experimental instantaneous depolymerization velocity distribution. We have obtained the best fits (black full line in Fig. 5 of the main paper) with $v_1/v_o = 30 \pm 5$ for both guanosine-5'-[(β, γ)-methyleno]triphosphate (GMPCPP) and GTP plus glycerol buffers. Instead the values found for L are 30 ± 6 for GMPCPP, whereas for GTP plus glycerol the experimental results are better fit using $L = 15 \pm 4$, in good accordance with the fact that shorter filaments may move similar distances in a more viscous medium than longer filaments in the aqueous buffer. These values for v_1 and L may only be considered as semiquantitative predictions because the specific choice of the parameters in Eq. **S24** is reasonable but by no means unique, and the fit to the experimental data leave large error bars. Nevertheless, the qualitative interpretation of the depolymerization as random fragmentations with an enhanced frequency for short fragments is very robust and well founded.

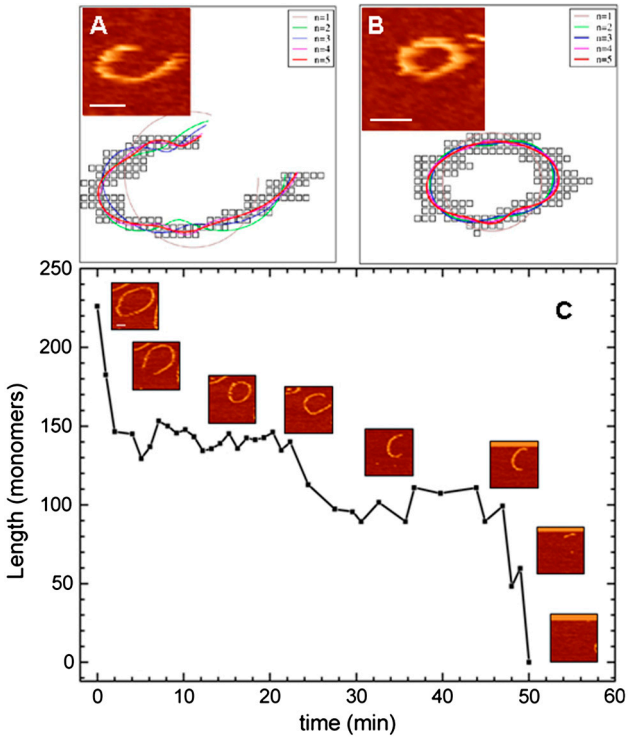

Fig. S1. Fitted curves for a FtsZ ring and filament using different harmonics. *A* and *B* show the fit to the digitalized image for different value of *n*. *C* illustrates the time evolution of the filament length estimated from the AFM images. (Scale bars: 100 nm.)

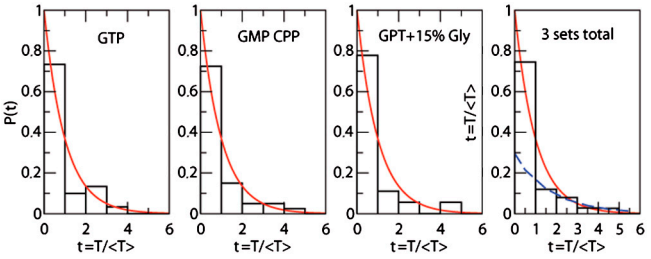

Fig. S2. Normalized histograms for the survival time of FtzS rings in different nucleotide buffers. The time is scaled with the mean value $\langle T \rangle$ for each set. The red lines correspond to the exponential decay $P(\tau) = \exp(-\tau)$ predicted by Eq. **S3**. The blue dashed line is a one exponential fit that illustrates that one exponent can only account for the slow tail but not the behavior of the full histogram.

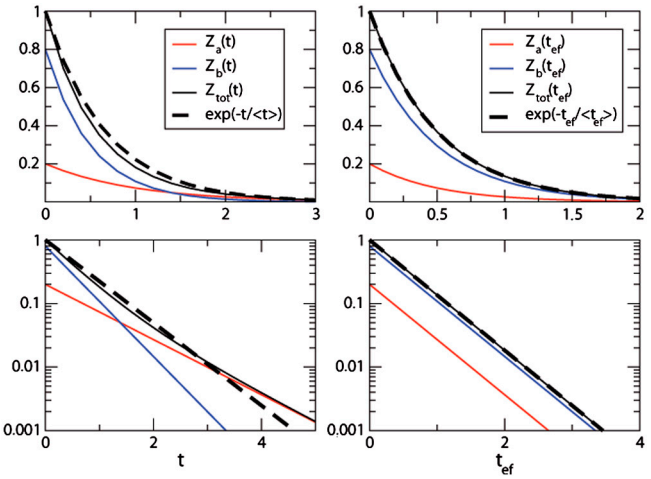

Fig. S3. At the left-hand side, the continuous black line is the distribution $Z_{\text{tot}}(t)$ for the survival times in a system with two subpopulations: *a* (red line) with initial concentration $P_a(0) = 0.2$ and reaction rate $k_a = 1$ (in arbitrary units), and *b* (blue line) with $P_a(0) = 0.8$ and $k_b = 2$. The dashed line is the exponential distribution that would describe a single process with the mean reaction rate. The log scale (*Lower*) shows more clearly the tail of the distributions. At the right-hand side, the same data are analyzed in terms of the effective time, which takes into account the ratio $k_b/k_a = 2$ and produces a pure exponential decay for $Z_{\text{ef}}(t_{\text{ef}})$.

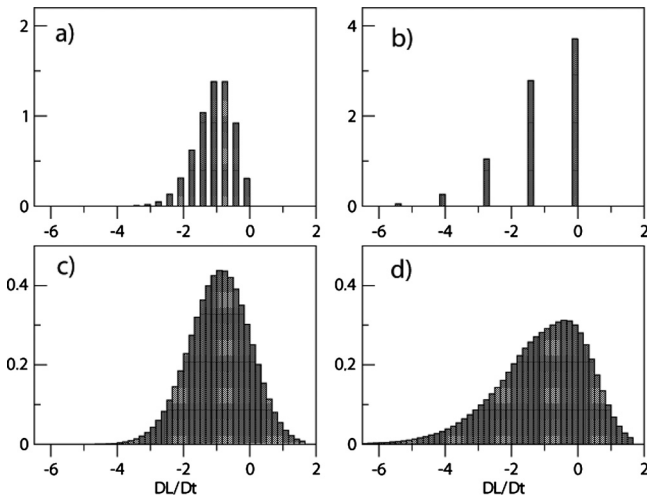

Fig. S4. The distribution of chain length that would be observed in the simple examples described here. *A* is the Poisson distributions for one-by-one depolymerization events Eq. **S21**; *B* represents Eq. **S22** for the hypothetical four-by-four depolymerization. Both cases have the same mean value (taken as arbitrary unit), and they correspond to observations times relatively large, $\Delta_t = 3$, so that every "observed" change of length may include several "depolymerization events." With the ideal resolution of these graphs, the difference between the two cases would be obvious: *A* presents nonzero probabilities for all the values corresponding to an integer number of monomers, whereas in *B* the gap between observed values for "instantaneous" depolymerization rates is four times larger. In the bottom distributions, we have added a Gaussian noise to the results, so that the gaps between observed rates have disappeared. Nevertheless, the shape of the distributions still allows one to distinguish between the one-by-one (*A* and *C*) and the four-by-four (*B* and *D*) cases.

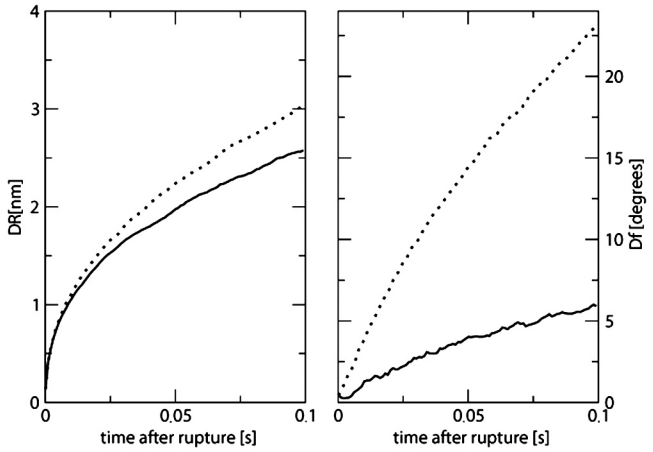

Fig. S5. The standard deviation for the distribution of distances (*Left*, in nanometers) and relative angle (*Right*, in degrees) between the ends of a broken bond in a set of Langevin simulations for model FtsZ filaments. The growth of ΔR and $\Delta\phi$ with the time (in seconds) after the breaking of a polymeric bond along the filament reflects the diffusive changes in the shapes of the filaments (see text). The full lines correspond to the fragmentation of a filament with $N = 100$ monomers into two equal pieces ($N_a = N_b = 50$). Other fragmentations with $N_a \neq N_b$ give similar results unless one of the pieces is very small. The dotted lines correspond to the separation of a single monomer ($N_a = 1$, $N_b = 99$), which shows faster diffusion in distance and particularly in the relative angle.

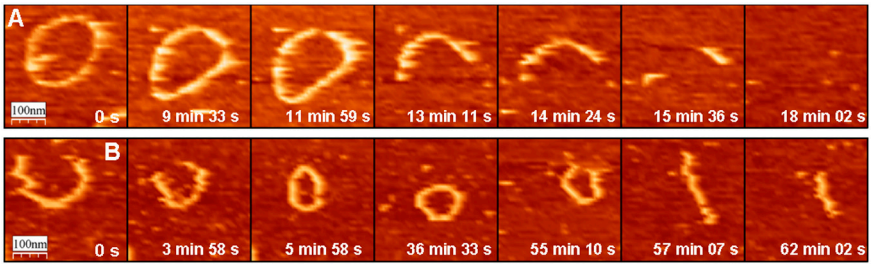

Fig. S6. The figure shows the time evolution of FtsZ filaments imaged in acid buffers: (*A*) pH 6.5, (*B*) pH 5.0.

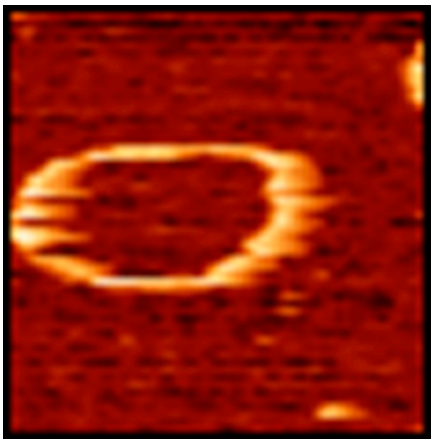

Movie S1*A*. The behavior of closed rings formed with GTP.

Movie S1*A* (AVI)

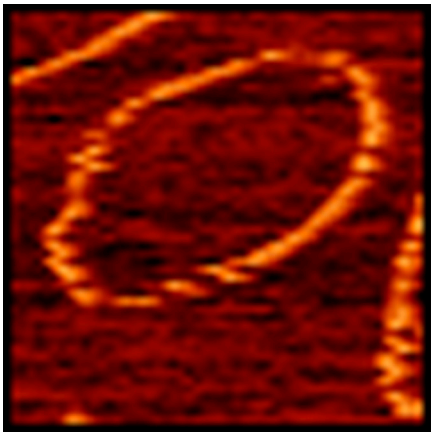

Movie S1*B*. The behavior of closed rings containing GMPCPP.

Movie S1*B* (AVI)

Movie S2*A*. The evolution of an open filament containing GMPCPP.

Movie S2*A* (AVI)

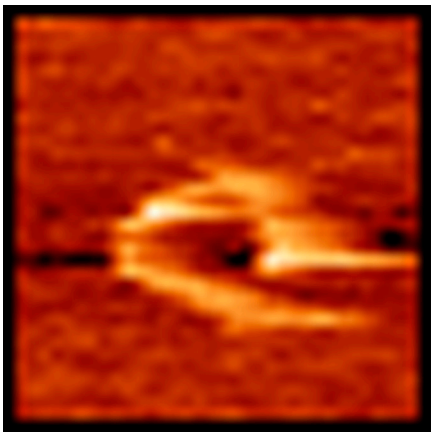

Movie S2*B*. The evolution of a filament containing GTP imaged in a buffer containing 15% glycerol.

Movie S2*B* (AVI)

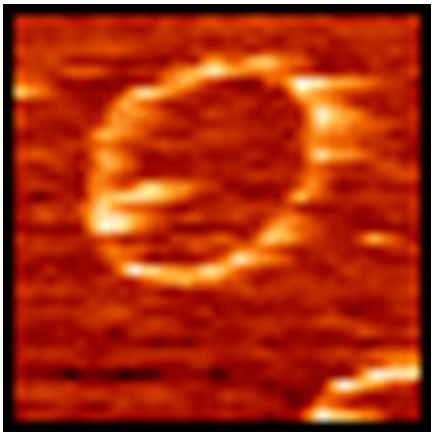

Movie S3*A*. The evolution of a filament containing GTP imaged in a buffer at pH 6.5.

Movie S3*A* (AVI)

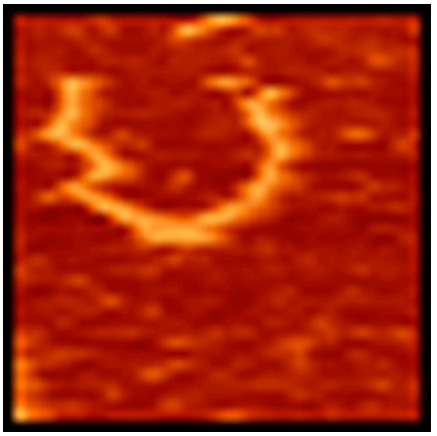

Movie S3*B*. The evolution of a filament containing GTP imaged in a buffer at pH 5.

Movie S3*B* (AVI)

Table S1. The number of observed FtsZ rings, their mean size and size dispersion, and the mean time for which each ring is observed, with GTP buffers of different acidity

pH	7.5	6.5	5.0
No. rings	243	176	69
$\langle N \rangle$	103	99	80
σ_N	26	28	16
$\langle T \rangle$, min	6.5	22.0	25.5
$\langle T_b \rangle$, min	670	2,200	2,000
v_o, min^{-1}	0.0015	0.00045	0.0005